Hindawi
Journal of Food Biochemistry
Volume 2024, Article ID 5520236, 18 pages
https://doi.org/10.1155/2024/5520236

Research Article

Development of Sustainable Vegan Pea Protein-Zinc Complex: Characterization, *In Vitro* Cellular Mineral Uptake, and Application in Functional Biscuit Production

Aprjita Jindal,[1] Nikhil Dnyaneshwar Patil,[1] Aarti Bains,[2] Minaxi Sharma,[3] Anil Kumar,[4] Nemat Ali,[5] Prince Chawla,[1] and Kandi Sridhar[6]

[1]*Department of Food Technology and Nutrition, Lovely Professional University, Phagwara 144411, India*
[2]*Department of Microbiology, Lovely Professional University, Phagwara 144411, India*
[3]*Department of Applied Biology, University of Science and Technology Meghalaya, Baridua 793101, India*
[4]*Department of Food Science Technology and Processing, Amity University, Mohali 140306, India*
[5]*Department of Pharmacology and Toxicology, College of Pharmacy, King Saud University, Riyadh 11451, Saudi Arabia*
[6]*Department of Food Technology, Karpagam Academy of Higher Education (Deemed to Be University), Coimbatore 641021, India*

Correspondence should be addressed to Prince Chawla; princefoodtech@gmail.com and Kandi Sridhar; sridhar4647@gmail.com

Received 24 August 2023; Revised 17 January 2024; Accepted 7 May 2024; Published 20 May 2024

Academic Editor: Naciye Kutlu

This study aimed to investigate the potential of pea protein concentrate (PPC) to form protein-mineral composites, with a specific focus on its zinc- (Zn-) binding capabilities. In addition, the physical and functional properties of PPC were evaluated. PPC, a potential protein source, was found to possess lipophilic properties, suggesting its suitability for various applications in food production. The investigation involved a comprehensive characterization of pea protein concentrate-zinc complex (PPC-Zn) composites, utilizing various analytical techniques such as Fourier transform infrared spectroscopy, scanning electron microscopy, particle size analysis, zeta potential measurement, and thermogravimetric analysis. The findings of this study indicated that the protein content of PPC-Zn (79.02 ± 1.33%) insignificantly increased as compared to PPC (78.86 ± 1.16%). Furthermore, PPC demonstrated improved functional properties, including increased protein solubility (2.55%), enhanced water-holding (13.09%) and oil-holding capacity (11.17%), and improved foaming capacity and stability (2.08% and 6.07%, respectively). These improvements in functional properties were likely attributed to the unique surface structure observed in SEM micrographs. The research also highlighted the maximum binding capacity of PPC for zinc, which was observed at concentrations of 5 mM (95.35 ± 1.86%). This binding of zinc ions to PPC induced changes in the characteristics and internal structures of the protein concentrate. Notably, the presence of functional groups such as -COOH, -OH, and $-NH_2$ in PPC suggested their involvement in coordinating with zinc ions to form PPC-Zn composites. This investigation demonstrated a significant increase (2.26%) in the mineral bioavailability of PPC-Zn. Additionally, the cellular uptake, retention, and transport of PPC-Zn were improved by 9.79%, 7.84%, and 9.51%, respectively. Fortified biscuits (B2) demonstrated enhanced cellular uptake (2.79%), retention (4.84%), and transport (3.51%) compared with control biscuits. Fortified biscuits (B2) had higher microbial counts (total plate count is 3.57 ± 0.03 and the yeast-mold count is 3.96 ± 0.07 cfu/g) than control biscuits (B1) (total plate count is 2.49 ± 0.13 and the yeast-mold count is 3.44 ± 0.11 cfu/g) at the end of storage, and there is no difference in sensory evaluation between the control and fortified biscuits. Furthermore, the key findings indicated that PPC could serve as a promising carrier for mineral supplements, binding with zinc effectively.

1. Introduction

In the current era, there is a growing global concern about the widespread occurrence of micronutrient deficiencies, which have significant negative impacts on various age groups and result in adverse health consequences. In particular, pregnant women and children under the age of 5 are highly vulnerable to deficiencies in essential minerals such as iron, zinc, calcium, magnesium, and copper [1]. These vital nutrients are regulated by factors including dietary habits, food intake, mineral absorption, and recycling processes within the human body. Inadequate levels of minerals can lead to the development of severe diseases and disorders, directly or indirectly affecting physiological processes, such as compromised tissue oxygen delivery, weakened physical strength, cognitive impairment, reduced productivity, and increased susceptibility to infections [2]. Zinc deficiency, for instance, can impair cellular signaling, mitochondrial respiration, and intermediary metabolism and may contribute to congenital anomalies, prenatal growth retardation, compromised immune function, and cognitive impairment [3]. The recognition of the importance of addressing micronutrient deficiencies has significantly increased among governmental, nongovernmental, and industrial entities in recent years. However, diversifying diets to alleviate mineral deficiencies is often hindered by factors such as affordability, availability, and religious constraints [4]. Moreover, certain foods contain antinutritional properties that affect the absorption of minerals, thereby contributing to deficiencies in the human body. Consequently, food fortification with external sources of minerals has been identified as an effective strategy by the World Health Organization (WHO) and the Food and Agriculture Organization (FAO), utilizing existing distribution systems within the food industry [5].

Traditionally, several inorganic salts have been added to fortify food products with minerals, playing a crucial role in factors such as bioavailability, chemical stability, appearance, and uniformity of the fortified products. These inorganic salts have served as a sustainable and economic alternative in combating mineral deficiencies and ensuring the nutritional security of large populations for many years [6]. However, recent studies have revealed various drawbacks associated with inorganic minerals, such as zinc sulfate due to their toxic effects, raising concerns about their severe impact on human health. Long-term use of inorganic minerals has been observed to lead to toxicity as they accumulate in the human body [7]. The resulting tissue-level toxicity can range from mild symptoms such as nausea and abdominal pain to severe health problems such as liver abnormalities and increased intracranial pressure [4]. Additionally, the presence of inorganic minerals in their free form can induce extreme toxicity by generating reactive oxygen species, while excessive long-term use can result in metabolic acidosis [8]. The accumulation of free zinc ions in the human brain has been linked to neurotoxicity. As a result, recent studies have explored alternative approaches involving the interaction of minerals with proteins to form complexes, thereby mitigating the use of inorganic minerals [9]. The study by Shilpashree et al. [10] showed that complexing iron or zinc with whey protein (WP) reduces iron's pro-oxidant activity and increases the bioavailability of both minerals. WP-mineral complexes protected against oxidative stress and provided favorable conditions for mineral absorption compared to free minerals. Moreover, Caco-2 cells exhibited significantly higher bioavailability of iron and zinc when delivered as WP-mineral complexes. The research conducted by Shilpashree et al. [11] demonstrated that Fe- and Zn-bound sodium caseinate (S.NaCas) have higher binding capacities than uncomplexed minerals. This binding resulted in altered physicochemical properties of the complexes, including changes in solubility, surface charge, and molecular size. Notably, the Fe-bound S.NaCas complex showed significantly higher mineral uptake in Caco-2 cells compared with free Fe. Additionally, it promoted greater intracellular iron storage as measured by ferritin formation. Zn-bound S.NaCN also exhibited improved mineral uptake compared with free Zn.

The incorporation of zinc into protein-based food products has the potential to positively impact their shelf life and oxidative stability. Zinc, an essential trace element, exhibits antioxidant properties and can serve as a cofactor for enzymes involved in scavenging free radicals [12]. This antioxidant activity contributes to the prevention of oxidation in fats and other susceptible components. Additionally, zinc's interaction with proteins can enhance their overall stability, preventing denaturation and degradation over time [13]. The antimicrobial properties of zinc further inhibit the growth of spoilage microorganisms and pathogens, extending the product's shelf life. However, challenges such as metal-induced oxidation and maintaining optimal concentrations must be carefully addressed [14]. Strategies to overcome these challenges include the use of chelating agents, packaging with barrier properties, pH control, and the incorporation of synergistic antioxidants [15]. By navigating these considerations, the addition of zinc to proteins can be optimized to harness its beneficial effects on shelf life and oxidative stability without compromising product quality [16].

The development of a sustainable vegan pea protein concentrate-zinc complex offers a promising approach to address the growing demand for protein while minimizing environmental impact and promoting human health [17]. Pea protein production, compared with its animal-based counterparts, boasts a significantly reduced environmental footprint, requiring less land, water, and fertilizer, while simultaneously generating lower greenhouse gas emissions [18]. Moreover, the complexation of zinc with pea protein effectively enhances zinc bioavailability, addressing potential nutritional deficiencies prevalent in plant-based dietary patterns. The incorporation of this complex into functional food products, such as biscuits, not only provides enhanced nutritional value but also maintains sensory attributes, ensuring consumer acceptability [19]. By promoting the substitution of animal-based protein sources with vegan pea protein concentrate-zinc complexes, we can effectively mitigate the environmental impact of animal agriculture, reduce our reliance on animal resources, and contribute to the establishment of a more sustainable and healthier food system [20]. In addition to the abovementioned benefits, the utilization of vegan pea protein concentrate-zinc complexes aligns with the principles of circular economy, promoting resource efficiency and waste reduction. Pea protein, a byproduct

of pea starch production, would otherwise be discarded, representing a valuable resource left untapped [21]. By transforming this byproduct into a functional ingredient, we not only minimize waste generation but also add value to the pea processing chain, fostering sustainable practices within the food industry [22]. Furthermore, the incorporation of vegan pea protein concentrate-zinc complexes into food products can contribute to addressing global protein malnutrition, particularly in developing regions [23]. Pea protein, as a complete protein source, offers a viable alternative to animal-based proteins, providing essential amino acids for optimal growth and development. By increasing the availability of plant-based protein sources, we can enhance food security and promote nutritional well-being, particularly among vulnerable populations [24].

In the current study, we investigated the potential of pea protein concentrate (PPC) in forming protein-mineral composites, with a specific focus on zinc. Through this investigation, valuable insights into the physical, functional, and binding properties of PPC are expected to be gained, opening up possibilities for its utilization in the development of mineral-enriched food products. Previous studies have indicated that proteins from legumes, including those present in PPC, frequently bind with metal ions through functional groups such as carboxyl groups in Glu and Asp, imidazole groups in His, and sulfhydryl groups in Cys. The abundance of these binding sites in PPC along with its complex structure resulting from interactions such as hydrogen bonding and sulfide bridges, make it an excellent ligand for ferrous and zinc ions through multidentate coordination. Furthermore, the addition of inorganic salts to various food products has posed challenges, causing changes in sensory attributes and rendering them less acceptable for human consumption. For example, sensory analysis of several inorganic minerals, including gluconate, zinc sulfate, and chloride, revealed metallic taste, astringency, glutamate sensation, and bitterness, compromising their acceptability [25]. Therefore, this study will also assess the sensory attributes of biscuits fortified with PPC-Zn composites, aiming to overcome these sensory issues. To the best of our knowledge, despite extensive research on proteins derived from legumes in recent years, the zinc-binding abilities of proteins in a pea protein concentrate and their characterization, as well as the further development of composite biscuits based on PPC-Zn, have not yet been investigated.

2. Materials and Methods

2.1. Materials. Vegan protein source such as PPC was procured from Roquette India Pvt. Ltd., located in Ahmedabad, Gujarat, India. The food-grade minerals such as zinc sulfate monohydrate ($ZnSO_4{\cdot}H_2O$) were procured from Sigma-Aldrich, St. Louis, MO, USA. The other reagents used were Folin and Ciocalteu's reagent, sodium carbonate, copper sulfate, sodium potassium tartrate, bovine serum albumin (BSA), sodium hydroxide, and phosphate buffer, and other general chemicals used in this study were procured from Laboratory Reagents and Fine Chemicals, Loba Chemie Pvt. Ltd., Mumbai, India. Ingredients used for biscuit preparation involved refined wheat flour, powdered sugar, butter, vanilla essence, baking soda, and salt and were purchased from the local market in Phagwara, Punjab. The study used acid-washed class "A" certified glassware throughout the experimentation, and all the reagents and standard solutions were prepared using triple-distilled water.

2.2. Methods

2.2.1. Preparation of Protein-Zinc Complex (PPC-Zn) and Fortified Biscuits. (1) Preparation of PPC-Zn. The zinc-binding capacity of PPC was assessed through ultrafiltration (UF), following the methodology described by Patil et al. [26]. Solutions of PPC were prepared at a concentration of 0.01 g/mL. Zinc was incrementally introduced to each protein solution at concentrations spanning from 1 to 10 mmol/L. This addition was executed under constant agitation using a magnetic stirrer. The pH of the protein-zinc complex was set at 6.5, and the complex was subsequently incubated for a duration of 2 h at a temperature of 24°C, to optimize the interaction between zinc and protein. After centrifugation at $14000 \times g$ for 30 min at 24°C, the supernatant containing soluble protein and zinc was diligently separated and subsequently underwent further processing via the utilization of Amicon ultrafiltration (UF) membrane tubes featuring a molecular weight cut-off of 10 kDa. The collected filtrate underwent analysis to quantify its zinc content using the inductively coupled plasma-optical emission spectrometry (ICP-OES) technique (Toshvin Analytical Pvt. Ltd., Mumbai, Maharashtra, India). Subsequent to this, a pilot-scale UF membrane system was deployed to generate PPC-Zn. A diafiltration procedure was applied to ascertain the presence of free zinc in the gathered filtrate. In particular, 2 mL of 4 M NaOH was added to 20 mL of collected filtrate, followed by centrifugation to acquire a solution devoid of pellets. Lastly, the concentrate was reduced to a quarter of its initial volume and subsequently subjected to spray drying. The zinc retention and yield in protein-zinc complexes were calculated according to the following equations:

$$\text{Zinc retention (\%)} = \left[\left(\frac{\text{The concentration of zinc in the complex}}{\text{Amount of zinc concentration added}}\right) \times 100\right], \quad (1)$$

$$\text{Yield (\%)} = \left[\left(\frac{\text{Weight of obtained complex (g)}}{\text{Weight of added protein source (g)}}\right) \times 100\right]. \quad (2)$$

The ultrafiltration (UF) procedure was executed utilizing a Sartorius ultrafiltration unit, furnished with a Masterflex Easy-Load pump-7518. The filtration process employed a Hydrosart membrane featuring a molecular weight cut-off of 10 KDa and a filtration surface area measuring 0.1 m^2. The membrane's pressure setting was calibrated to 15 psi, while the cross-flow velocity was sustained at 300 mL/min. To oversee the progress of the filtration process, flow meters and pressure gauges were strategically interconnected to the inlet and outlet points of both the permeate and retentate streams of the membrane.

(2) Preparation of Biscuits. The procedure for biscuit preparation, encompassing both the control and fortified variants, adhered to a consistent set of operational steps with specific differentiations attributed to the introduction of fortification materials. The control biscuit formulation, following the method outlined by Santosh et al. [27] with minor adaptations, involved a meticulous integration of refined wheat flour, powdered sugar, butter, vanilla essence, baking soda, and salt. The mixture of dry ingredients, namely, refined wheat flour, powdered sugar, baking soda, and salt, transpired within a designated mixing vessel. The infusion of softened butter and vanilla essence followed, prompting manual blending to yield a coherent dough matrix. Subsequent to the dough's preparation, a resting period coincided with the oven preheating to an established temperature of 100°C, for 10 min. After this preparatory phase, the dough underwent controlled rolling to achieve an approximate thickness of 0.635 cm, facilitated by a lightly floured surface. The implementation of a biscuit cutter yielded distinct biscuit units, which were subsequently transferred onto a baking sheet and subjected to a controlled baking process at 140°C for a time span ranging between 15 and 20 min. Verification of proper internal baking was ascertained through the use of a toothpick. After baking, the biscuits were cooled, stored in vacuum-sealed pouches, and labeled "B1." In alignment with the methodological framework established, the fortification phase was introduced, implicating the incorporation of specific composite materials. The integration of zinc fortification was facilitated through the use of zinc sulfate monohydrate, individually denoted PPC-Zn composites. The composite-based biscuit formulation followed an analogous procedure to the control variant, with distinct adjustments attributed to the introduction of 1.0 g of the respective composite powders within each dough. Following this incorporation, the subsequent kneading process homogenized the components. The doughs were subject to a comparable resting period concurrent with the oven preheating at 100°C over a 10-min interval. Consistent with the prior methodology, the doughs were uniformly rolled out and biscuit units were delineated through a biscuit cutter. Baking of the fortified biscuits occurred at 140°C for 15–20 min, culminating in an externally observed light golden-brown hue. Verification of internal completeness of baking was again conducted through a toothpick assessment. The post-baking cooling duration was consistently observed, prior to the finalized storage within the vacuum-sealed pouches, denoted as B2.

2.2.2. Analysis of the Pea Protein concentrate-Zinc Complex and Fortified Biscuits

(1) Protein Content. The Folin–Lowry method was employed to determine protein content in a sample following the Lowry et al. [28] procedure. A sample preparation involved dissolving 1.0 g of pea protein concentrate powder in 100 mL of distilled water to obtain a 1% protein solution. After adding reagents and vortexing, test tubes were incubated for 30 min at room temperature in the dark. Color intensity was measured at 660 nm, and a standard curve relating concentrations to absorbance was generated using bovine serum albumin. The sample protein content was determined by interpolation. The protein content was estimated using the following equation:

$$\text{Protein Content } (\mu\text{g/mL}) = \text{Concentration of protein from standard curve} \times \text{dilution factor}. \quad (3)$$

(2) Estimation of Zinc Content. The zinc content within PPC was evaluated according to the methodology outlined in the investigation conducted by Absulijabbar et al. [29]. For quantitative zinc analysis using ICP-OES (inductively coupled plasma-optical emission spectrometry), glass laboratory dishes were immersed in 10% nitric acid (HNO_3) for 24 h, followed by cleaning with deionized water and air-drying. ICP-OES was calibrated via ICAL (Intelligent Calibration Logic) based on 2012 SPECTRO Analytical Instruments GmbH guidelines. A calibration curve was generated by diluting a standard solution with water for targeted zinc concentrations, using nine data points. Zinc analysis at the 213.8 nm emission line utilized radial plasma observation. The procedure excluded flux or hydrochloric acid, simulating sample fusion matrix preparation. Concentrations above 10 mg/L yielded a precipitate, attributed to chloride anions. The initial verification calibration (ICV) control sample was a 20 mg/L zinc solution, adhering to ±10% deviation from expected values for validation, following 2012 SPECTRO Analytical Instruments GmbH and 2014 U.S. EPA recommendations. Control sample analysis occurred after every ten-sample sequence to ensure measurement precision and reliability.

(3) Mineral Binding Efficiency. The zinc-protein mineral binding efficiency was determined according to the following equation given by Shilpashree et al. [30]:

$$\text{Mineral binding efficiency (\%)} = \left[\left(\frac{\text{The total amount of zinc present in the sample}}{\text{The free form of zinc present in the sample}}\right) \times 100\right]. \quad (4)$$

(4) Functional Properties

(1) Protein Solubility (PS)

Solubility is one of the most commonly measured functional properties of food proteins. The analysis of the solubility of the PPC sample was conducted using the following method by Li et al. [31]. Sample (1 g) was dissolved in 100 mL of phosphate buffer (0.05 M, pH 7), and the pH of the solution was adjusted to 7 using 0.1 N NaOH. The solution in a beaker was mixed for 1 hr with the help of a magnetic stirrer at 30°C followed by centrifugation at 18000 × g for 20 min at 4°C. The supernatant was filtered through Whatman No. 1 filter paper, and protein content was determined using Lowry's method. The percentage of solubility was calculated as follows:

$$\text{Protein solubility (\%)} = \left[\left(\frac{\text{Protein concentration in the supernatant}}{\text{Total protein concentration in the sample}}\right) \times 100\right]. \quad (5)$$

(2) Water-Holding Capacity and Oil-Holding Capacity (WHC and OHC)

The water-holding and oil-holding capacities of the PPC were determined using the method outlined by Li et al. [32]. Firstly, the weight of the centrifuge tubes was measured and a sample (1 g) was added to it, and again, the weight of the centrifuge tube was measured. Then, the sample was mixed with 10 mL of distilled water for WHC or 10 mL of canola oil for OHC in a preweight centrifuge tube. The mixture was allowed to stand for 30 min to reach equilibrium and then centrifuged at 2000 × g for 15 min. The excess water/oil was carefully decanted, and the remaining wet protein mass was weighed. The water-holding and oil-holding capacities were calculated as the ratio of the mass of water retained to the initial mass of the sample, expressed as a percentage.

(3) Foaming Capacity and Stability

The foaming capacity and stability of pea protein concentrate powder were examined according to the method of Li et al. [32]. A sample (1 g) was incorporated into 50 mL of triple-distilled water. Employing a magnetic stirrer at 500 rpm, stirring persisted for 30 min until a uniform solution was formed. The soluble fraction was gathered to evaluate foaming attributes. After centrifugation at 10000 rpm for 15 min, the sample was vigorously blended at maximum speed using an electric blender for 10 min. The resulting foam was promptly transferred to a 100 mL measuring cylinder, and initial and final volumes were recorded. Foam capacity, indicating volume percentage increase, and foaming stability, denoting volume change after 30 min at room temperature, were calculated. The percentage change in volume was computed to measure the foaming capacity. The foaming capacity was calculated using the following equations:

$$\text{Foaming capacity (\%)} = \left[\left(\frac{\text{Whipped volume (mL)} - \text{Initial volume (mL)}}{\text{Initial volume (mL)}}\right) \times 100\right]. \quad (6)$$

The change in foam volume after 30 min (30°C) was measured as foam stability and was determined using the following equation:

$$\text{Foaming stability (\%)} = \left[\left(\frac{\text{Volume after resting (mL)} - \text{volume before resting (mL)}}{\text{Volume before resting (mL)}}\right) \times 100\right]. \quad (7)$$

(5) Characterization of PPC-Zn Composites

(1) Scanning Electron Microscope (SEM)

The SEM of the PPC-Zn was measured according to the method described by Relucenti et al. [33]. Morphological characteristics of powdered pea protein were evaluated using a field emission scanning electron microscope (FE-SEM: JEOL JSM-7610F Plus, Tokyo, Japan) equipped with an energy dispersive detector (EDS: MRB EDS, SDD 150 LN2 Free, UK) and a Gold Sputter Coater (ACG World Smart Coater). An amount of 5 mg of pea protein powder was affixed to carbon-coated copper tape. Gold coating, achieved via a sputtering process at 30 mA for 2 min, was executed to improve conductivity. Micrographs were acquired at magnifications of 500X, 2000X, 25000X, and 5000X, utilizing accelerating voltages of 15 and 20.0 kV. Consistent working distance at 8.0–7.9 mm was upheld across all magnifications.

(2) Thermogravimetric Analysis (TGA)

Thermal stability and mass variation of pea protein powder were assessed employing TGA (TGA 340 Em Prepash, Scinco Co. Ltd., Korea) using the method described by Saadsatkhah et al. [34]. Test specimens (15 mg) underwent controlled heating from 10 to 950°C at a steady pace (10°C/min) under a nitrogen environment (50 ml/min), while monitoring weight loss for thermal characterization.

(3) Fourier Transform Infrared Spectroscopy (FTIR)

The FTIR of the PPC-Zn was evaluated according to the method described by Tiernan et al. [35]. FTIR was employed to investigate functional groups in pea protein powder using ATR and pellet accessories (PerkinElmer X400). A sample mixture was prepared by combining 10 mg pea protein powder with 100 mg KBr, and the mixture was deposited onto a pristine machine mirror surface. Data collection spanned 4000 to 400 cm^{-1}, utilizing air as the background. Transmittance data were acquired and managed using Spectrum 10 software.

(4) Particle Size and Zeta Potential

The particle size and zeta potential of the PPC-Zn were examined using the methodology described by Li et al. [36]. The zeta potential and size of pea protein were determined using a particle size and zeta potential analyzer (Microtrac MRB NANOTRAC Wave II, Osaka, Japan) at 24°C. A 1% solution of each protein type was prepared and subjected to ultrasonication in an ultrasonic water bath for 10 min.

(6) Mineral Bioavailability

(1) *In Vitro* Mineral Bioavailability

Pea protein concentrate-zinc bioavailability was assessed using the procedure of He et al. [37]. The method simulated digestion and used Caco-2 cells to gauge absorption, providing insights into its nutritional impact.

(2) Stimulated Gastrointestinal Digestion

Pea protein concentrate-zinc complex bioavailability was assessed using the procedure of He et al. [37]. The experiment mimicked gastrointestinal digestion, aiming to understand zinc absorption and its nutritional implications. In the simulation, 5 mL of protein mixed with 1.90 mL of saliva was agitated at 35°C and 95 rpm for 10 min. Gastric digestion was followed by 3.1 mL of gastric juice (pH adjusted to 2) incubated at 35°C for 2 h. Subsequently, a mixture of 1.97 mL of bile and 5.30 mL of duodenal juice was added, simulating intestinal digestion for 3 h. After digestion, ultrafiltration separated soluble and insoluble components. Zinc bioavailability was calculated from the soluble fraction of zinc concentration using the following equation, estimating the available zinc for absorption in PPC:

$$\text{Zinc bioavailability (\%)} = \left[\left(\frac{\text{Zinc concentration of dialysate (permeate)}}{\text{Zinc concentration of the sample}}\right) \times 100\right]. \quad (8)$$

(3) Cellular Absorption Study (Transwell Assay)

Caco-2 cells were cultured according to Jiang et al. [38]. The growth medium comprised 30 μg/mL streptomycin, 25 μg/mL amphotericin, 100 μg/mL penicillin, 2 mM L-glutamine, 10% heat-inactivated fetal bovine serum, and 1% DMEM (Dulbecco's modified Eagle's medium). Caco-2 cells were cultured at 35°C, 96% humidity, and 4% CO2. Medium renewal occurred every other day, with cell passage at around 90% confluence every 7–8 days using 0.05% EDTA (ethylenediaminetetraacetic acid) and 0.5% trypsin. For mineral absorption assays, Caco-2 cells from the 39th passage were seeded at 50,000 cells per 0.4 μm pore size in the 24 mm sterile polyester membrane-equipped well in six-well plates. Cells underwent further differentiation in a CO2 incubator, with PBS washing and medium refreshment every other day. Following 4–5 initial days, a 10-day differentiation period preceded the transepithelial cellular absorption assay.

(4) Evaluation of Cell Monolayer Integrity

Inverted light microscopy was routinely employed to evaluate Caco-2 cell morphology and identify contaminants. For assessing cell quality upon full coverage, the phenol red dye test was executed. After cell washing, the lower compartment contained 2 mL of PBS, while the upper compartment comprised 2 mL of phenol red dye-containing DMEM. Incubation followed, and 100 μl samples were collected from both compartments. Phenol red migration into the lower compartment was gauged using an automated ELISA plate reader (Beckman Coulter, Brea, CA) at 558 nm wavelength.

(5) Transport Studies of Mineral

Transepithelial mineral transport was examined by exposing rinsed Caco-2 cells to 2 mL of DMEM containing mineral dialysate acquired from simulated gastrointestinal treatment. The medium held a 50 μM mineral concentration and was placed in the upper wells, while 2 mL of regular DMEM occupied the lower compartments. Following a 3 hour incubation at 37°C, medium removal allowed for the assessment of transepithelial absorption. Subsequently, cells underwent a 22 hour culture to induce ferritin synthesis. Mineral transfer analysis utilized the ICP-OES technique, quantifying minerals in upper and lower cell culture compartments. This method enabled precise mineral quantification within the cellular barrier's context.

(7) Application

(1) Sensory Analysis

The sensory evaluation of biscuit samples was conducted using a nine-point hedonic scale, assessing attributes such as appearance, color, taste, texture, aroma, and overall acceptability. The panel comprised 30 members, evenly divided between 15 males and 15 females, with ages ranging from 23 to 45 years old. The sensory analysis was reviewed and approved by the institutional ethical committee with reference number LPU/CA/023/25/03/12026. The nine-point hedonic scale with 9—like extremely to 5—neither like nor dislike and 1—dislike extremely was used, and samples were coded with specific code numbers to avoid biasness. The selected formulations of biscuits were designated as B-1 (control) and B-2 (pea protein concentrate-zinc). The panelist evaluated biscuits for their appearance, color, taste, texture, aroma, and overall acceptability. All sensory assessments took place in the Food Technology and Nutrition Department of Lovely Professional University, Phagwara, Punjab, India.

(2) Microbial Analysis

Microbial assessment of the biscuits encompassed quantification of total plate count and yeast and mold count as per the methodology of Pokharel et al. [39]. Aseptic protocols were rigorously upheld to obviate extraneous contamination. Biscuit samples were meticulously prepared through sterile techniques and aseptically transferred to sterile containers. Serial dilutions employing sterile diluents were executed. For the total plate count, agar media of relevance were utilized, with subsequent spread plating of diluted samples. Incubation parameters, as stipulated, were adhered to. Following incubation, the discerning enumeration of colonies transpired, with their enumeration culminating in colony-forming units per gram (cfu/g) of biscuit. Analogously, yeast and mold quantification employed selective agar media, customized to these microorganisms' needs. Diluted samples were subject to spread plating, succeeded by incubation under specified conditions. Subsequent colony enumeration allowed for a distinction between yeast and mold colonies.

2.3. Statistical Analysis. Data were presented as the mean ± standard deviation (SD) of the triplicate samples. Statistical analysis was performed using SPSS software version 25.0 (IBM Inc., Chicago, IL, USA), and an independent-samples *t*-test was applied to compare the means between the biscuit samples at the 0.05 significance level.

3. Results and Discussion

3.1. Zinc-Binding Efficiency of PPC. As shown in Figure 1, the mineral binding efficiency of the PPC increases significantly ($p \leq 0.05$) from 89.65 ± 1.26 to $95.35 \pm 1.86\%$ up to the addition of 1–5 mM concentration of zinc sulfate in the protein and reaches its maximum at 5 mM concentration of zinc ($95.35 \pm 1.86\%$). This increase can be attributed to the presence of specific amino acids and charged side chains within PPC. Since zinc ions carry a positive charge in their ionic form, the negatively charged key amino acids (such as Glu, Asp, Arg, and Gly) present in PPC tend to form ionic bonds, contributing to the formation of complexes with high binding efficiency [40]. This phenomenon is supported by previous studies indicating that zinc binds to pea protein through various amino groups, including amide and carboxyl groups on the protein's side chain and specific functional groups such as imidazole and thiol. Furthermore, the morphological characteristics of the pea protein concentrate might have contributed to its maximum binding capacity and strong affinity for zinc ions [41]. In particular, the protein was found to possess a significant number of coordination sites on its surface, leading to a multidentate coordination pattern. The binding process was observed to be rapid and endothermic, indicating the spontaneous energy-absorbing nature of the interaction [42]. As the zinc concentration increases in the range of 5–12 mM, the mineral binding efficiency of PPC increases nonsignificantly ($p \geq 0.05$) (95.35 ± 1.86 to $96.04 \pm 0.20\%$). This could be attributed due to the saturation of binding sites, altered protein conformation, competitive binding with other ions, pH and ionic changes, solubility limits, and potential protein

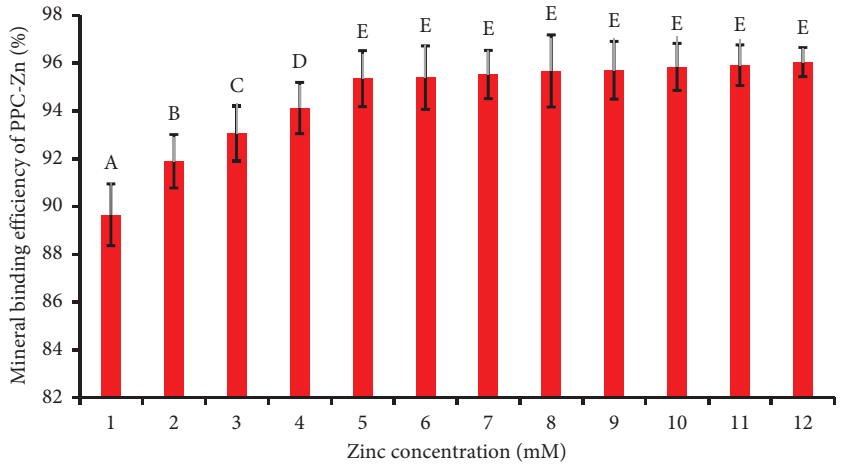

Figure 1: Mineral binding efficiency of the PPC-Zn (pea protein concentrate-zinc complex). The results were expressed as the mean ± standard deviation of ≥3 independent replicates, and error bars represent the standard deviation from the mean values, while different uppercase letters above each bar represent significantly different values within samples based on the analysis of the *t*-test.

aggregation. Additionally, elevated zinc sulfate concentrations could facilitate protein-protein interactions, impacting site accessibility and binding efficiency [43]. Our study aligns with Shilpashree et al. [44], who found maximum zinc-binding capacity at 2 mM Zn concentration.

Protein samples with the highest zinc-binding capacities, including pea protein concentrate bound with zinc at 5 mM (PPC-Zn), were selected for further investigation. This concentration was chosen due to a statistically significant increase in zinc-binding capacity observed up to this concentration. Beyond this concentration (5 to 12 mM), a nonsignificant increase in the mineral binding efficiency was observed. A comprehensive analysis will assess their functional properties and characteristic features. *In vitro* mineral bioavailability studies will determine the availability of bound zinc for human body absorption, and cellular mineral uptake of zinc will be examined to evaluate the proteins' efficiency in delivering zinc to cells.

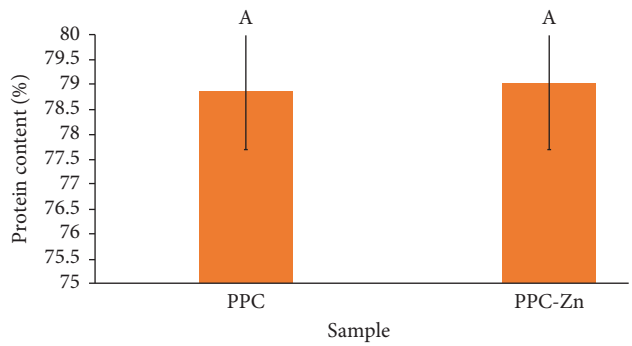

Figure 2: Protein content of PPC and PPC-Zn. PPC-Zn, pea protein concentrate-zinc complex; PPC, pea protein concentrate. The results were expressed as the mean ± standard deviation of ≥3 independent replicates, and error bars represent the standard deviation from the mean values, while different uppercase letters above each bar represent significantly different values within samples based on the analysis of the *t*-test.

3.2. Protein Content of PPC and PPC-Zn. As shown in Figure 2, the protein content of PPC-Zn (79.02 ± 1.33%) shows a nonsignificant difference ($p \geq 0.05$) as compared to PPC (78.86 ± 1.16%). The nonsignificant increase is due to the nature of the zinc-binding interactions, which could involve weak affinities that do not significantly alter the overall protein structure. Additionally, the proportion of protein molecules engaged in the zinc-binding process might be relatively small, resulting in an overall limited effect on the protein content [45].

3.3. Characterization of PPC-Zn and PPC

3.3.1. Scanning Electron Microscope (SEM). As shown in Figure 3(a), the SEM analysis conducted on the pea protein concentrate-zinc complex revealed important structural insights into the interaction between pea protein and zinc ions. In the SEM images, distinct morphological changes were observed in the pea protein samples after zinc complexation compared with the native pea protein. The native pea protein exhibited a relatively smooth and uniform surface under SEM, consistent with its native structure. However, upon complexation with zinc ions, the surface morphology exhibited variations. Irregularities, including small aggregates or clusters, were noticeable on the surface of the pea protein concentrate-zinc complex. This suggests that zinc binding might induce some degree of protein aggregation or conformational changes. The observed structural alterations could be attributed to the binding of zinc ions to specific amino acid residues on the pea protein, leading to changes in intermolecular interactions. These changes might affect the protein's overall conformation and surface characteristics, ultimately influencing its aggregation behavior [46]. The surface irregularities and aggregates suggest that zinc binding induces localized structural rearrangements within the protein matrix [42]. These findings align with previous studies indicating that metal ion binding can influence protein structure and interactions [30].

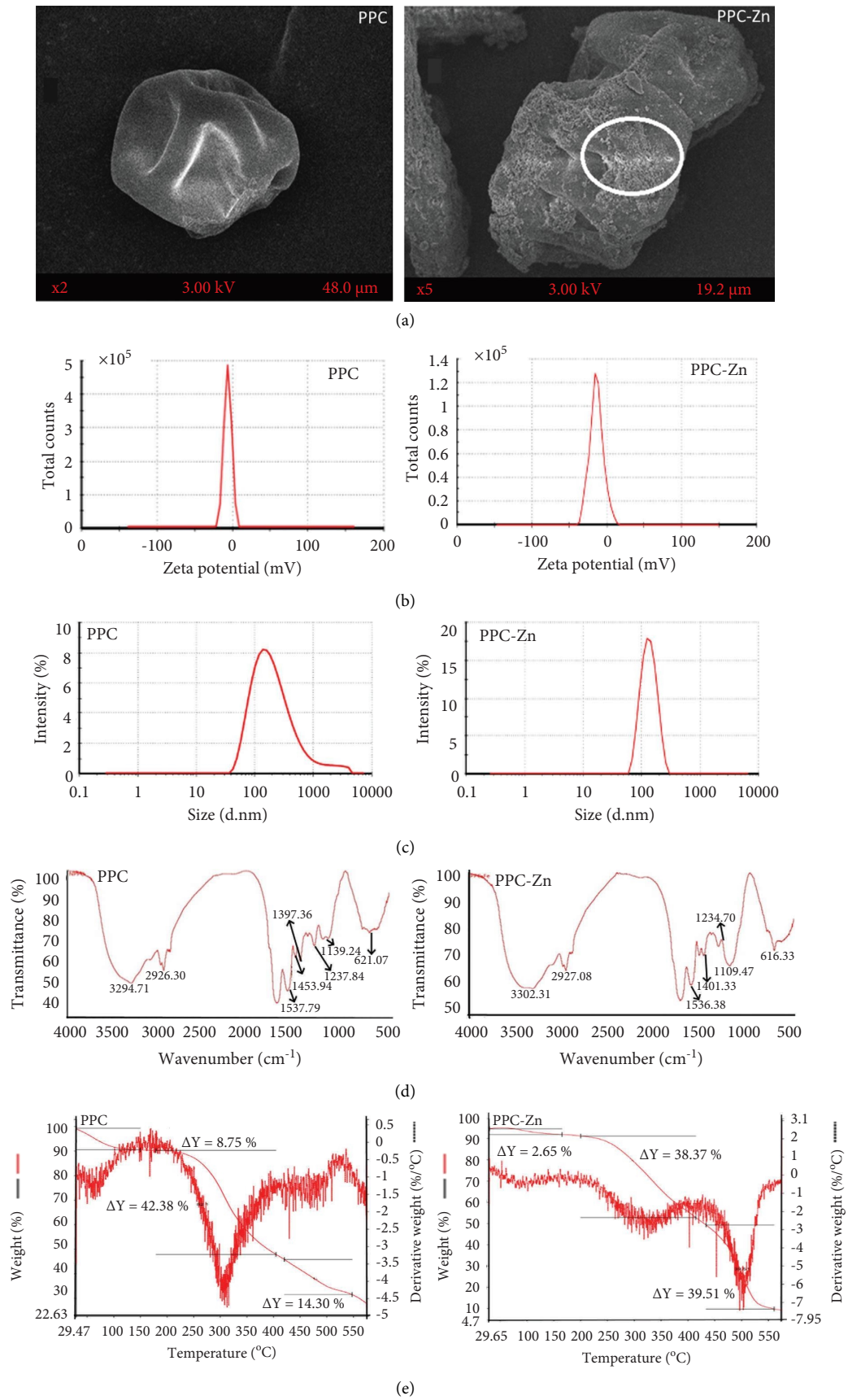

FIGURE 3: (a) SEM, (b) zeta potential, (c) particle size, (d) FTIR, and (e) TGA of the PPC and PPC-Zn. PPC-Zn, pea protein concentrate-zinc complex; PPC, pea protein concentrate; SEM, scanning electron microscopy; FTIR, Fourier transform infrared; TGA, thermogravimetric analysis.

3.3.2. Particle Size and Zeta Potential. As represented in Figure 3(b), the zeta potential value of the PPC-Zn (-13.86 ± 0.23 mV) shows a significant difference ($p \leq 0.05$) as compared to the PPC (-10.89 ± 0.31 mV). This observation suggests that the introduction of zinc ions induces a significant change in the overall surface charge of the protein. This could imply that the binding of zinc makes a significant impact on the electrostatic interactions at the protein's surface [47]. Similarly, as shown in Figure 3(c), the particle size of PPC-Zn (226.76 ± 0.45 nm) shows a nonsignificant difference ($p \geq 0.05$) compared with PPC (221.76 ± 0.45 nm) (Figure 2(c)). This result suggests that zinc coordination at the studied concentrations does not markedly alter the protein's colloidal stability or induce noticeable aggregation effects.

3.3.3. Fourier Transform Infrared (FTIR). The FTIR spectra provide valuable insights into the structural changes, as shown in Figure 3(d), which occur in PPC-Zn and PPC. In the spectral region associated with O-H stretching vibrations, the wavenumbers of 3294.711 cm^{-1} and 3302.131 cm^{-1}, indicative of hydroxyl groups, exhibit a slight difference. This discrepancy might be attributed to the interaction between zinc ions and hydroxyl groups within the protein, suggesting potential modifications in the protein's hydrogen bonding network. The C-H stretching vibrations, represented by wavenumbers of 2926.346 cm^{-1} and 2927.087 cm^{-1}, display minimal variance between PPC and PPC-Zn. This suggests that the fundamental carbon-hydrogen bonds, prevalent in aliphatic hydrocarbons, remain relatively unaffected by the binding of zinc ions. The wavenumbers of 1537.793 cm^{-1} and 1536.382 cm^{-1}, corresponding to amide II vibrations arising from N-H bending and C-N stretching interactions, exhibit a slight difference. This could imply subtle conformational changes in the protein structure upon zinc binding, potentially affecting its overall stability and functional properties. Observing the wavenumbers of 1435.945 cm^{-1} and 1450.399 cm^{-1} associated with CH_2 bending vibrations reveals the potential for alterations in the secondary structure of the protein due to zinc binding. Similarly, the variations in wavenumbers of 1397.363 cm^{-1} and 1401.339 cm^{-1}, reflecting CH_3 bending vibrations, further suggest structural adjustments induced by the binding process. The region featuring wavenumbers of 1237.845 cm^{-1} and 1234.701 cm^{-1}, possibly linked to C-N stretching vibrations within the peptide backbone, might indicate broader modifications to the protein's overall structure as a consequence of zinc binding. In the spectral range involving C-O stretching vibrations, the wavenumbers of 1139.247 cm^{-1} and 1109.474 cm^{-1}, corresponding to carbonyl groups, show differences that hint at changes in the secondary structure of the protein upon zinc interaction. Finally, the fingerprint regions with wavenumbers of 621.072 cm^{-1} and 616.335 cm^{-1} represent a diverse set of functional group contributions. Alterations in these regions may provide insights into shifts within the overall molecular environment of the pea protein due to zinc binding.

Comparing the overall intensity of the peaks, it is noticeable that some peaks, such as the one at 1109.474 cm^{-1}, exhibit significant changes in intensity upon zinc binding. This could indicate alterations in the protein's secondary structure and bonding environment caused by the coordination of zinc ions [48]. Additionally, zinc ions are known to play crucial roles in stabilizing protein structures and influencing their functions. The variations in peak positions and intensities suggest local conformational adjustments and alterations in hydrogen bonding patterns in the protein upon zinc coordination [49].

3.3.4. Thermogravimetric Analysis (TGA). As depicted in Figure 3(e), the thermogravimetric analysis of both PPC and PPC-Zn revealed distinct thermal degradation characteristics across different temperature ranges. In the low-temperature range (150 to 250°C), both PPC and PPC-Zn exhibited comparable weight losses, with delta Y values of approximately 8.75% and 2.65%, respectively. This similarity suggests that the initial weight loss is primarily due to the evaporation of moisture and volatile compounds present within the samples. Moving into the intermediate temperature range (400 to 450°C), both samples experienced significant weight loss, as indicated by substantial delta Y values of 42.38% for PPC and 38.35% for PPC-Zn. This stage corresponds to the decomposition of protein structures and the release of volatile organic fragments. Even at higher temperatures in the range of 500 to 550°C, both PPC and PPC-Zn continued to exhibit weight loss, with delta Y values of 14.30% and 39.51%, respectively. This weight loss can be attributed to the degradation of residual organic matter and the potential formation of ash content.

The subtle variations in weight loss observed between PPC and PPC-Zn across the studied temperature intervals suggest that zinc binding has a minimal impact on the overall thermal stability of pea protein. The consistent degradation patterns imply that the coordination of zinc ions does not induce significant alterations in the molecular structure of the protein, thereby maintaining its thermal behavior [50].

3.4. Functional Properties of the PPC and PPC-Zn

3.4.1. Protein Solubility (PS). As represented in Figure 4(a), the protein solubility of PPC-Zn significantly increases ($p \leq 0.05$) from 79.83 ± 1.23 to 81.92 ± 1.36%, which is enhanced by 2.55% as compared to PPC. The significant increase in protein solubility due to the structural changes induced by zinc coordination likely favors interactions with the solvent molecules. Zinc binding could disrupt certain internal protein interactions, potentially unfolding compact regions and making them more accessible to water molecules [51]. Additionally, the coordination of zinc ions might alter the distribution of charges across the protein's surface. This charge rearrangement can impact the protein's interactions with surrounding water molecules. If the exposed hydrophilic regions of the protein increase due to zinc coordination, more water molecules can surround and solvate the protein, further contributing to its improved solubility [52].

3.4.2. Water-Holding Capacity and Oil-Holding Capacity (WHC and OHC). According to Figure 4(b), the WHC and OHC of the PPC-Zn significantly increased ($p \leq 0.05$) by

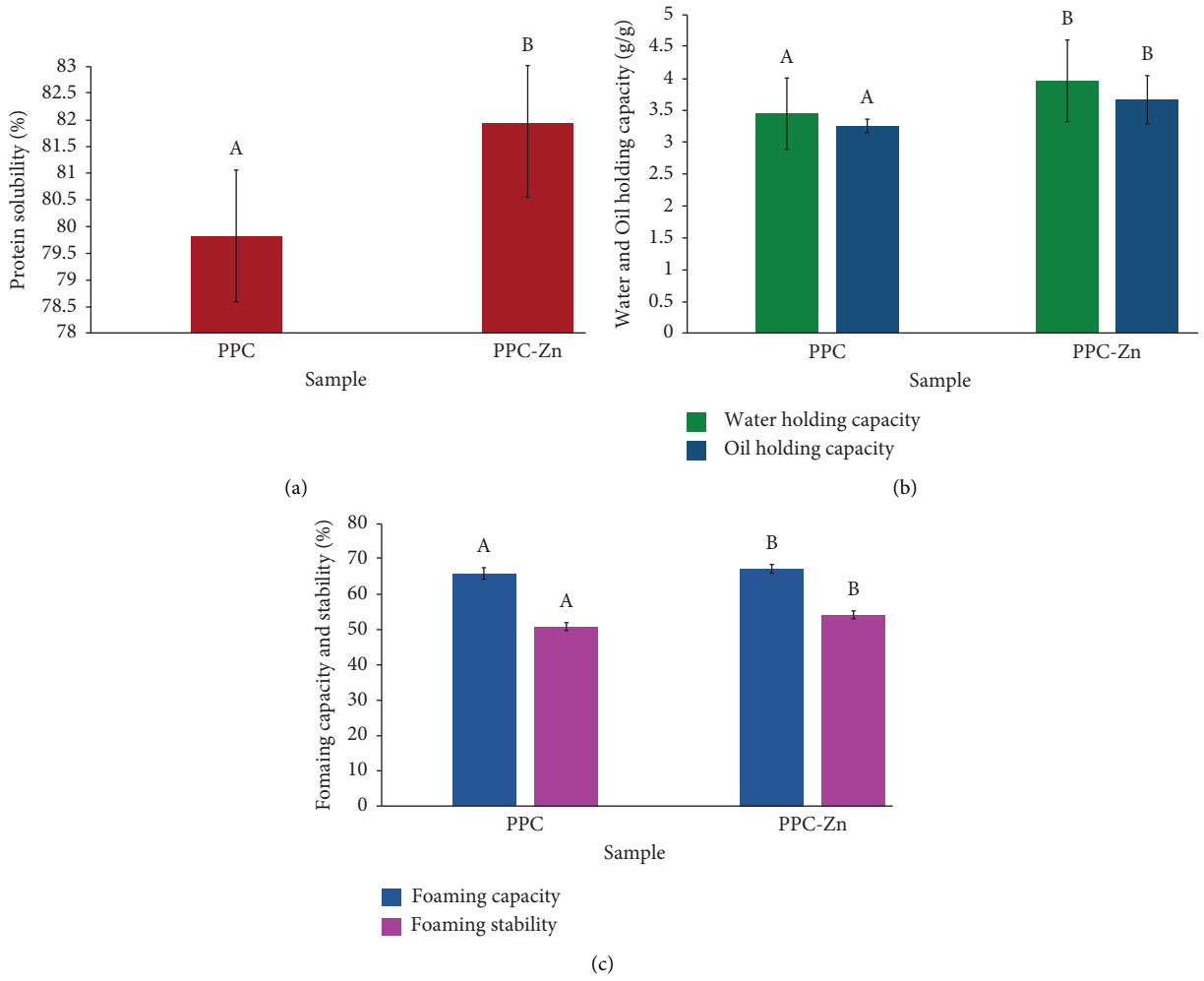

Figure 4: (a) Protein solubility, (b) water- and oil-holding capacities, and (c) foaming capacity and foaming stability of the PPC and PPC-Zn. The results were expressed as the mean ± standard deviation of ≥3 independent replicates, and error bars represent the standard deviation from the mean values, while different lowercase letters above each bar represent significantly different values within samples based on *t*-tests. PPC-Zn, pea protein concentrate-zinc complex; PPC, pea protein concentrate.

13.09% (3.45 ± 0.57 g/g to 3.97 ± 0.63 g/g) and 11.17% (3.26 ± 0.11 g/g to 3.67 ± 0.38 g/g) as compared to PPC. The observed improvement in WHC and OHC of PPC-Zn compared with PPC can be attributed to the interactions between zinc ions and the protein's structure. This interaction potentially leads to enhanced hydration properties as a result of zinc's coordination. The binding of zinc ions might induce conformational changes within the protein, creating more favorable binding sites for water molecules. This conformational adaptation is believed to contribute to the heightened water-holding capacity of the protein [53]. Similarly, the increased OHC observed in PPC-Zn can be attributed to the influence of zinc ions on the protein's interactions with oil molecules. The presence of zinc ions seems to enhance the protein's affinity for oil components. This could be facilitated by modifications in the protein's surface properties caused by the binding of zinc ions. These modifications likely result in more effective interactions between the protein and oil, leading to improved oil retention [54].

3.4.3. Foaming Capacity and Foaming Stability (FC and FS). As shown in Figure 4(c), the FC and FS of the PPC-Zn significantly increased ($p \leq 0.05$) by 2.08% (65.89 ± 1.54 to 67.29 ± 1.23%) and 6.07% (51.03 ± 1.12 to 54.33 ± 1.06%) as compared to PPC. This enhancement is likely attributed to altered intermolecular interactions facilitated by zinc binding, potentially leading to enhanced protein unfolding and increased surface activity. Consequently, greater protein availability at the air-water interface promotes the creation of stable foams [55]. Furthermore, the improved stability observed in foams generated from PPC highlights the contribution of zinc ions in reinforcing the protein network at the air-water interface. The coordination of zinc ions potentially fosters cross-linking or electrostatic interactions that strengthen cohesive forces within the protein matrix,

resulting in enhanced resistance to foam collapse over time [56].

3.5. Zinc Content. As illustrated in Figure 5(a), the zinc content of the PPC-Zn significantly increased ($p \leq 0.05$) by 9.86% as compared to zinc sulfate. The increased zinc content observed in PPC-Zn can be attributed to a combination of factors arising from the binding process between zinc ions and the protein structure. Chelation, a critical mechanism in this process, involves the bonding of zinc ions with specific amino acid residues within the pea protein structure. This chelation not only enhances the stability of the resulting complex but also prevents the undesirable precipitation or aggregation of zinc ions [57]. As a result, the chelated zinc ions remain tightly associated with the pea protein, leading to elevated zinc retention and concentration. Furthermore, the interaction between zinc ions and the pea protein molecule induces structural changes that hold potential significance [58]. These structural modifications may uncover previously concealed amino acid residues, thus creating new interaction sites for zinc ions. The consequential adjustments in the protein's folding pattern and secondary structure contribute to the formation of additional binding sites for zinc [59]. Our investigation concurs with the findings of Shilpashree et al. [10], where the zinc bioavailability of whey protein-zinc complex increased by 9.26% as compared to whey protein.

3.6. Zinc Bioavailability. As shown in Figure 5(b), the zinc bioavailability of PPC-Zn is $74.22 \pm 0.37\%$, which significantly increases ($p \leq 0.05$) by 2.26% as compared to zinc sulfate. This can be attributed to several factors that interact to enhance the absorption and utilization of zinc by the human body. Firstly, pea protein contains naturally occurring compounds such as phytic acid, which acts as an antinutrient by binding to minerals such as zinc, limiting their absorption in the gut [60]. However, during the processing of pea protein, techniques such as enzymatic hydrolysis or fermentation are often employed. These processes can break down antinutritional factors such as phytic acid, reducing their inhibitory effects on mineral absorption. Moreover, the protein matrix of pea protein may create a favorable environment for zinc absorption. The amino acids present in the protein can potentially form complexes with zinc, aiding in its solubilization and subsequent uptake in the small intestine [61]. This interaction could protect the zinc from binding with other compounds that might inhibit absorption. However, zinc sulfate, although a common dietary zinc source, can present absorption challenges. It dissociates into ionic zinc in the digestive tract, which can compete with other minerals for absorption sites. Additionally, the ionic nature of zinc sulfate might expose it to interactions with dietary components that can reduce its absorption or bioavailability [62]. Our study demonstrates concurrence with the investigation conducted by Shilpashree et al. [10]. Their work revealed that the zinc bioavailability of whey protein increased by 13.15%.

3.7. Zinc Uptake by Caco-2 Cells. As depicted in Figure 5(c), the cellular transport, retention, and uptake of the PPC-Zn significantly increase ($p \leq 0.05$) by 9.79% (23.39 ± 0.63 to $25.93 \pm 0.69\%$), 7.84% (30.65 ± 0.45 to $33.26 \pm 0.93\%$), and 9.511% (55.94 ± 0.34 to $61.82 \pm 0.48\%$) as compared to zinc sulfate. The significant increase in cellular transport, retention, and uptake of PPC-Zn compared with zinc sulfate can be attributed to several interrelated factors that collectively create a more favorable environment for zinc absorption and utilization within the body's cells. Firstly, the protein matrix of pea protein plays a pivotal role [63]. The amino acids present in the protein can form chelation complexes with zinc ions. This chelation enhances the solubility of zinc, preventing its precipitation and aggregation in the gastrointestinal tract, and facilitates its transport through the intestinal mucosa into the bloodstream. The chelated form of zinc is more stable and less likely to interact with other dietary components that might inhibit absorption or reduce its bioavailability [64]. Furthermore, the protein-bound zinc can be recognized by specific transporters on the surface of intestinal cells. These transporters are designed to recognize and transport amino acid complexes, which allow the zinc to be more efficiently taken up by the enterocytes. This recognition mechanism can lead to a higher rate of absorption for protein-bound zinc compared with the ionic form found in zinc sulfate [65]. Once absorbed, the zinc bound to pea protein might also have advantages in terms of cellular retention. The chelated form of zinc is less likely to be excreted directly through the kidneys, as it is shielded from the competitive ion transport systems that regulate renal excretion. This enhanced retention within the body can contribute to sustained zinc availability for cellular processes [66]. Additionally, the potential reduction in antinutritional factors within pea protein through processing can further contribute to increased cellular uptake. Phytic acid, which is present in various plant-based foods, including peas, can hinder mineral absorption. Processing methods that break down phytic acid can alleviate this inhibition, making zinc more accessible for uptake into cells [67]. Our study correlates with the research of Shilpashree et al. [10], where they found that cellular transport, retention, and uptake of whey protein increase by 5.86%, 9.09%, and 7.70% as compared to zinc sulfate.

This experiment investigated the potential of protein-bound zinc for enhancing cellular absorption compared with free zinc. Using Caco-2 cells as a model for human intestinal cells, they evaluated the impact of pea protein concentrate (PPC-Zn) on zinc transport, retention, and uptake. The study revealed a significant increase in all three parameters for PPC-Zn compared with zinc sulfate, suggesting that the protein matrix in PPC-Zn facilitates chelation, improves transport mechanisms, reduces antinutrients, and enhances retention, ultimately leading to improved zinc bioavailability. These findings suggest that PPC-Zn may be a more effective form of zinc supplementation than conventional zinc sulfate, with potential benefits for human health.

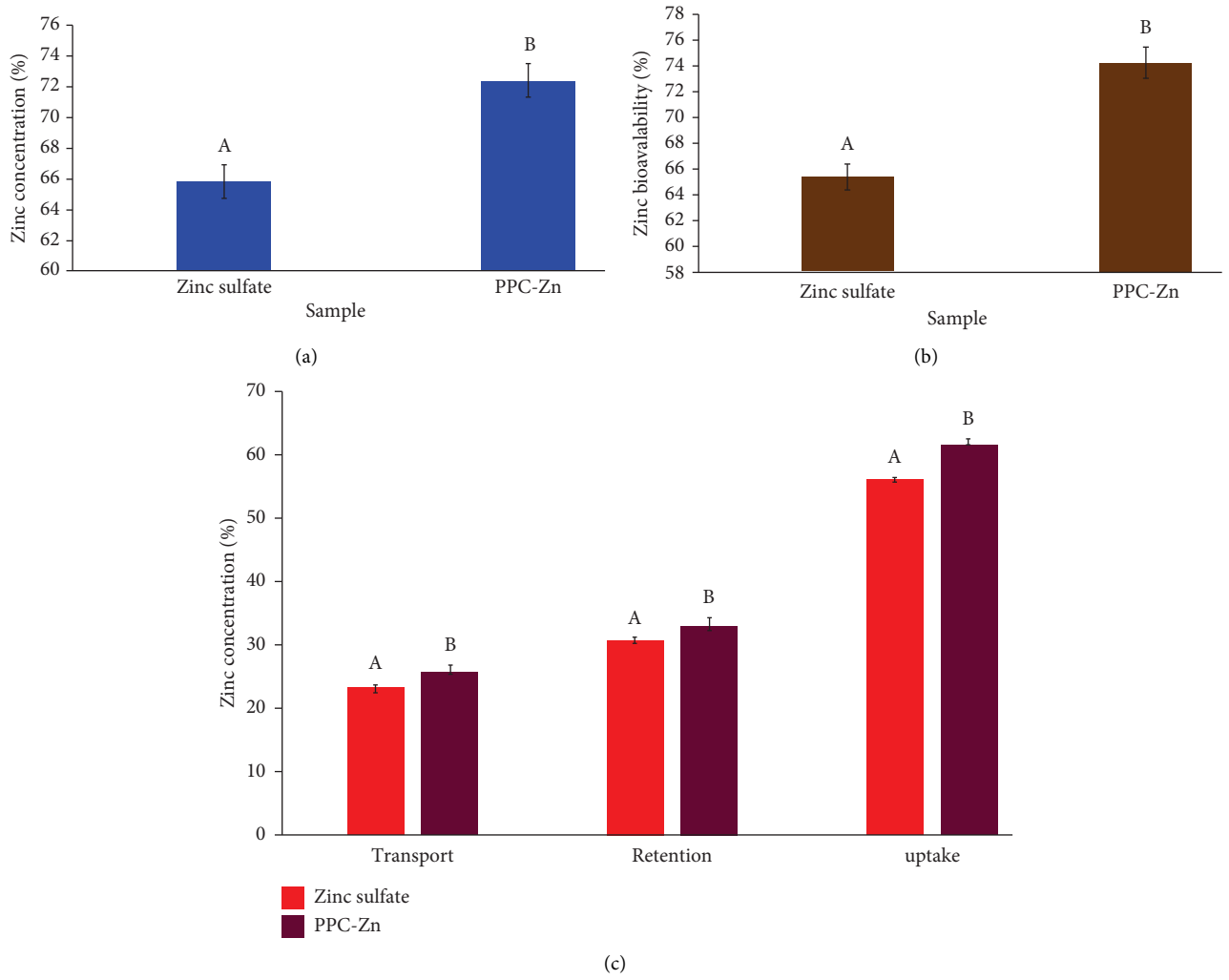

Figure 5: (a) Zinc content; (b) zinc bioavailability; and (c) cellular transport, retention, and uptake of the PPC-Zn. PPC-Zn, pea protein concentrate-zinc complex. The results were expressed as the mean ± standard deviation of ≥3 independent replicates, and error bars represent the standard deviation from the mean values, while different lowercase letters above each bar represent significantly different values within samples based on the analysis of the *t*-test.

Table 1: Microbiological analysis of pea protein protein-zinc powder-incorporated biscuits during the storage period.

Storage time (day)	Total plate count (cfu/g)		Yeast and mold count (cfu/g)	
	B1	B2	B1	B2
0	ND	ND	ND	ND
5	ND	ND	ND	ND
10	1.29 ± 0.07^{eA}	1.35 ± 0.11^{eB}	1.19 ± 0.14^{eA}	1.31 ± 0.13^{eB}
15	1.43 ± 0.12^{dA}	1.64 ± 0.53^{dB}	1.83 ± 0.06^{dA}	2.35 ± 0.05^{dB}
20	1.68 ± 0.11^{cA}	1.94 ± 0.21^{cB}	2.14 ± 0.05^{cA}	2.64 ± 0.11^{cB}
25	1.70 ± 0.15^{cA}	2.75 ± 0.09^{bB}	2.46 ± 0.08^{bA}	3.53 ± 0.06^{bB}
30	2.49 ± 0.13^{aA}	3.57 ± 0.03^{aB}	3.44 ± 0.11^{aA}	3.96 ± 0.07^{aB}

[1]Data are presented as the mean ± standard deviation of the triplicate samples. Means with different lowercase letters (a–e) within the column over the storage time and uppercase letters (A and B) within rows between the samples denote significant differences ($p \leq 0.05$) based on the *t*-test. B1 and B2: control biscuit and PPC-Zn powder-incorporated biscuit; PPC-Zn, pea protein concentrate-zinc complex; ND, not detected.

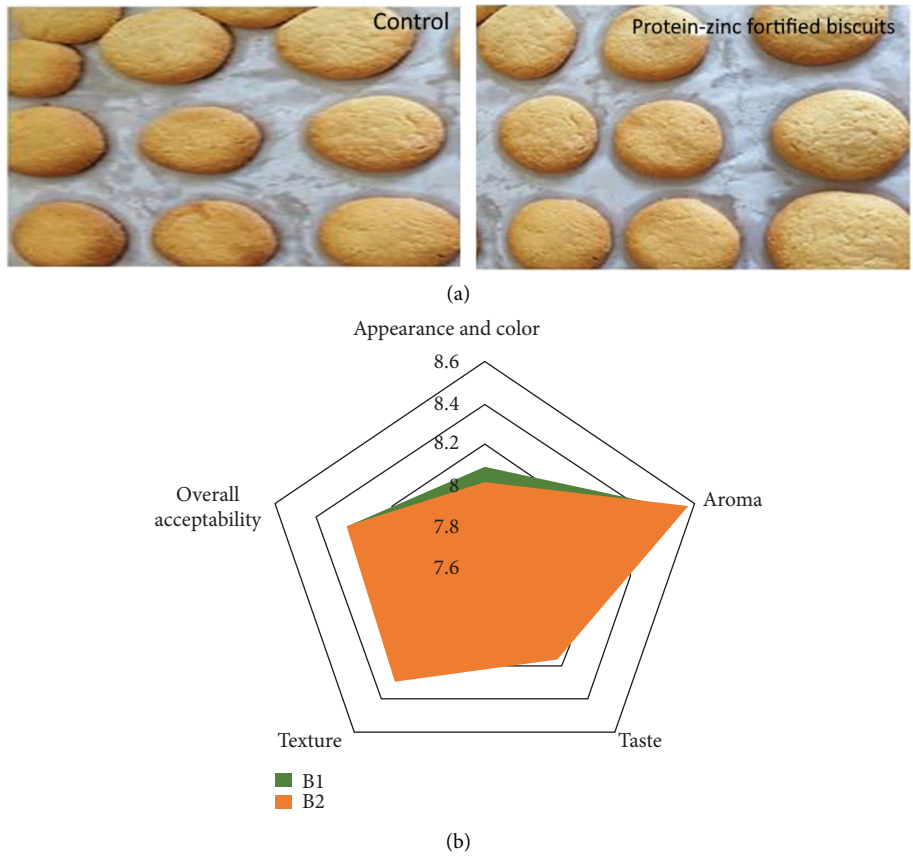

FIGURE 6: (a) Visual observation and (b) sensory analysis of biscuits. B1, control biscuit; B2, PPC-Zn powder-incorporated biscuits; PPC-Zn, pea protein concentrate-zinc complex.

3.8. Application

3.8.1. Microbial Analysis of Biscuits. Microbiological assessment of fortified biscuits (B2) and control samples (B1) during storage is shown in Table 1. The total plate count signifies the collective microbial burden within the samples. From day 0 to day 5 of storage, no microbial proliferation occurred in both B1 and B2 samples. Starting from day 10, a statistically significant discrepancy ($p \leq 0.05$) emerged between B1 and B2. In particular, the control (B1) exhibited a count of 1.29 ± 0.07 cfu/g, while B2 showed a slightly higher count of 1.35 ± 0.11 cfu/g. On days 15, 20, 25, and 30, notable distinctions ($p \leq 0.05$) were observed in the total plate count between B1 and B2. The counts escalated over time, with B2 consistently demonstrating elevated counts compared with B1. Similarly, on days 0 and 5, no yeast and mold proliferation was discernible in both B1 and B2. By day 10, a significant difference ($p \leq 0.05$) between B1 and B2 was evident. In particular, B1 displayed a count of 1.19 ± 0.14 cfu/g, while B2 exhibited a slightly higher count of 1.31 ± 0.19 cfu/g. On days 15, 20, 25, and 30, significant distinctions ($p \leq 0.05$) surfaced in the yeast and mold count between B1 and B2. Microbial counts rose during the storage duration, with B2 consistently manifesting greater counts than B1. In summary, the results underscore the impact of incorporating PPC-Zn powder on microbial growth. Throughout the storage timeframe, B2 consistently manifested elevated microbial counts compared with B1, albeit remaining within acceptable safety parameters.

3.8.2. Sensory Analysis of Biscuits. As represented in Figures 6(a) and 6(b), the comparative sensory analysis results between the fortified biscuit sample (B2) and the control (B1). The sensory attributes of the B2 sample exhibited a notable resemblance to those of the control sample. Sensory scores for both samples exhibited a decline with increasing storage duration. Over the 30-day storage investigation, discernible sensory alterations between B2 and control were absent from day 0 to day 15. Notably, color, flavor and taste, aroma, mouthfeel, and overall acceptability garnered panelists' approval for B2 over the control. Throughout the sensory analysis phase, both B2 and B1 samples were stored within aluminum zip lock pouches. B2's sensory traits remained consistent during the storage period of up to 15 days in comparison with the control. Beyond the 15-day mark, a marginal decrease in B2's sensory attributes became apparent in contrast to the control.

3.8.3. Zinc Uptake in Biscuits. As shown in Figure 7, the cellular transport, retention, and uptake of the PPC-Zn powder-incorporated biscuits significantly increase

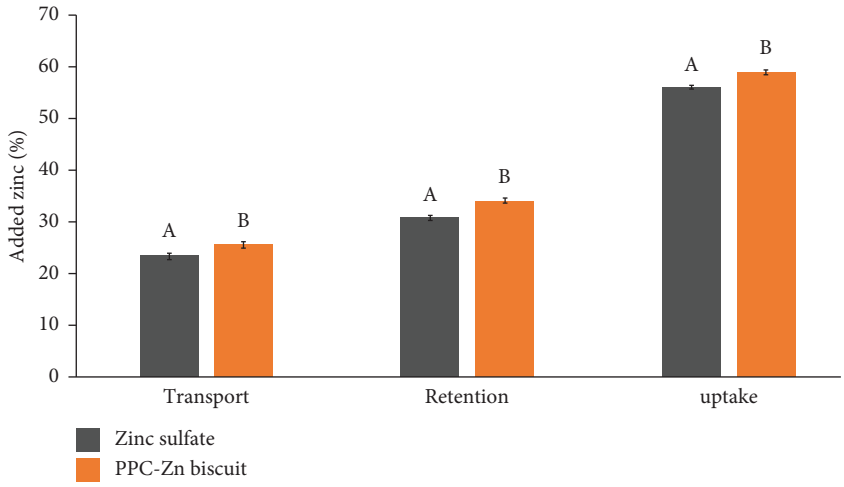

Figure 7: Cellular transport, retention, and uptake of the PPC-Zn powder-incorporated biscuits. The results were expressed as the mean ± standard deviation of ≥3 independent replicates, and error bars represent the standard deviation from the mean values, while different lowercase letters above each bar represent significantly different values within samples based on the analysis of the *t*-test. PPC-Zn, pea protein concentrate-zinc complex.

($p \leq 0.05$) by 8.41% (23.39 ± 0.63 to 25.54 ± 0.56%), 9.82% (30.65 ± 0.45 to 33.99 ± 0.39%), and 5.83% (55.34 ± 0.34 to 58.77 ± 0.48%) as compared to zinc sulfate. This increase is due to its superior bioavailability, solubility, and particle characteristics that facilitate efficient cellular interaction. PPC-Zn powder forms stable complexes, aiding absorption, and controlled release kinetics ensure sustained zinc supply, enhancing uptake. Synergistic effects with biscuit components further boost transport efficiency [68]. PPC-Zn powder's unique composition potentially improves digestibility, triggers specific cellular mechanisms, and promotes metabolic interactions, leading to effective zinc utilization. Its stability in the gastrointestinal environment supports absorption [49].

3.9. Limitations and Drawbacks. The study primarily focuses on the interaction between PPC and PPC-Zn, leaving unexplored potential interactions with other minerals, which could impact the broader utility of PPC. Additionally, the microbial counts in fortified biscuits were consistently higher than those in control biscuits throughout storage, highlighting the need for a more comprehensive examination of the long-term microbial stability and safety of the fortified product. Furthermore, the study does not extensively explore the impact of variations in processing conditions on the formation of PPC-Zn composites, and the economic feasibility of incorporating PPC-Zn into food products remains unaddressed. Clinical validation is essential to confirm the enhanced mineral bioavailability observed in PPC-Zn powder-incorporated biscuits in a human physiological context.

4. Conclusion

In conclusion, this study successfully developed a sustainable vegan pea protein concentrate-zinc (PPC-Zn) complex for the formulation of functional biscuits. The PPC-Zn complex exhibited improved functional properties, including solubility, water-holding capacity, oil-holding capacity, foaming capacity, and foaming stability. The PPC-Zn powder-incorporated biscuits exhibited acceptable sensory attributes and improved zinc bioavailability. The *in vitro* cellular mineral uptake studies demonstrated that the PPC-Zn complex was readily absorbed and retained by the cells. The findings of this study have significant implications for the development of functional food products to address the global challenge of zinc deficiency, particularly in vegan populations. The PPC-Zn complex is a promising functional ingredient that can be used to formulate a variety of food products, including biscuits, breads, pasta, and snacks. Future research should focus on evaluating the long-term stability of the PPC-Zn complex in food matrices and under different storage conditions. Additionally, clinical trials are needed to assess the efficacy of PPC-Zn powder-incorporated food products in improving zinc intake and status in humans. Overall, this study demonstrates the feasibility of developing sustainable vegan PPC-Zn complexes for the formulation of functional food products with improved zinc bioavailability.

Data Availability

All data generated or analyzed during this study are included in the manuscript.

Conflicts of Interest

The authors declare that they have no conflicts of interest.

Authors' Contributions

Aprjita Jindal and Nikhil Dnyaneshwar Patil contributed equally to this work.

Acknowledgments

This research was supported through the Researchers Supporting Project Number (RSPD2024R940), King Saud University, Riyadh, Saudi Arabia.

References

[1] N. Sa, F. Ea, B. Mm et al., "Nutrition in adolescent growth and development," *Yearbook of Paediatric Endocrinology*, vol. 399, pp. 172–184, 2022.

[2] S. M. T. Gharibzahedi and S. M. Jafari, "The importance of minerals in human nutrition: bioavailability, food fortification, processing effects and nanoencapsulation," *Trends in Food Science and Technology*, vol. 62, pp. 119–132, 2017.

[3] Y. Zhang, Y. Tian, H. Zhang, B. Xu, and H. Chen, "Potential pathways of zinc deficiency-promoted tumorigenesis," *Biomedicine and Pharmacotherapy*, vol. 133, Article ID 110983, 2021.

[4] J. R. N. Taylor, M. G. Ferruzzi, C. Ndiaye et al., "Entrepreneur-led food fortification: a complementary approach for nutritious diets in developing countries," *Global Food Security*, vol. 36, Article ID 100674, 2023.

[5] N. Pathaw, K. S. Devi, R. Sapam et al., "A comparative review on the anti-nutritional factors of herbal tea concoctions and their reduction strategies," *Frontiers in Nutrition*, vol. 9, Article ID 988964, 2022.

[6] A. Kumari and A. K. Chauhan, "Iron nanoparticles as a promising compound for food fortification in iron deficiency anemia: a review," *Journal of Food Science and Technology*, vol. 59, no. 9, pp. 3319–3335, 2022.

[7] V. Pal, G. Singh, and S. S. Dhaliwal, "A new approach in agronomic biofortification for improving zinc and iron content in chickpea (Cicer arietinum L.) grain with simultaneous foliar application of zinc sulphate, ferrous sulphate and urea," *Journal of Soil Science and Plant Nutrition*, vol. 21, no. 2, pp. 883–896, 2021.

[8] S. S. Shiek, S. T. Sajai, and H. S. Dsouza, "Arsenic-induced toxicity and the ameliorative role of antioxidants and natural compounds," *Journal of Biochemical and Molecular Toxicology*, vol. 37, no. 3, Article ID e23281, 2023.

[9] K. Raj, P. Kaur, G. D. Gupta, and S. Singh, "Metals associated neurodegeneration in Parkinson's disease: insight to physiological, pathological mechanisms and management," *Neuroscience Letters*, vol. 753, Article ID 135873, 2021.

[10] B. G. Shilpashree, S. Arora, S. Kapila, and V. Sharma, "Whey protein-iron or zinc complexation decreases pro-oxidant activity of iron and increases iron and zinc bioavailability," *Lebenson. Wiss. Technol.*, vol. 126, Article ID 109287, 2020.

[11] C. Gupta, S. Arora, M. A. Syama, and A. Sharma, "Physicochemical characterization of native and modified sodium caseinate-Vitamin A complexes," *Food Research International*, vol. 106, pp. 964–973, 2018.

[12] S. Gulzar, M. Tagrida, T. Prodpran, L. Li, and S. Benjakul, "Packaging films based on biopolymers from seafood processing wastes: preparation, properties, and their applications for shelf-life extension of seafoods-A comprehensive review," *Comprehensive Reviews in Food Science and Food Safety*, vol. 22, no. 6, pp. 4451–4483, 2023.

[13] M. Peng, Z. Tabashsum, M. Anderson et al., "Effectiveness of probiotics, prebiotics, and prebiotic-like components in common functional foods," *Comprehensive Reviews in Food Science and Food Safety*, vol. 19, no. 4, pp. 1908–1933, 2020.

[14] I. Kim, K. Viswanathan, G. Kasi, S. Thanakkasaranee, K. Sadeghi, and J. Seo, "ZnO nanostructures in active antibacterial food packaging: preparation methods, antimicrobial mechanisms, safety issues, future prospects, and challenges," *Food Reviews International*, vol. 38, no. 4, pp. 537–565, 2022.

[15] I. R. S. Vieira, A. P. A. d. de Carvalho, and C. A. Conte-Junior, "Recent advances in biobased and biodegradable polymer nanocomposites, nanoparticles, and natural antioxidants for antibacterial and antioxidant food packaging applications," *Comprehensive Reviews in Food Science and Food Safety*, vol. 21, no. 4, pp. 3673–3716, 2022.

[16] C. I. Colino, J. M. Lanao, and C. Gutierrez-Millan, "Recent advances in functionalized nanomaterials for the diagnosis and treatment of bacterial infections," *Materials Science and Engineering: C*, vol. 121, Article ID 111843, 2021.

[17] A. Green, C. Blattmann, C. Chen, and A. Mathys, "The role of alternative proteins and future foods in sustainable and contextually-adapted flexitarian diets," *Trends in Food Science and Technology*, vol. 124, pp. 250–258, 2022.

[18] W. R. Aimutis, "Plant-based proteins: the good, bad, and ugly," *Annual Review of Food Science and Technology*, vol. 13, pp. 1–17, 2022.

[19] Y. Y. Zhang, R. Stockmann, K. Ng, and S. Ajlouni, "Opportunities for plant-derived enhancers for iron, zinc, and calcium bioavailability: a review," *Comprehensive Reviews in Food Science and Food Safety*, vol. 20, no. 1, pp. 652–685, 2021.

[20] C. J. Bryant, "Plant-based animal product alternatives are healthier and more environmentally sustainable than animal products," *Future Foods*, vol. 6, Article ID 100174, 2022.

[21] J. Wilcox, *The Win-Win Diet: How to Be Plant-Based and Still Eat what You Love*, Post Hill Press, New York, NY, USA, 2022.

[22] F. Boukid, C. M. Rosell, and M. Castellari, "Pea protein ingredients: a mainstream ingredient to (re) formulate innovative foods and beverages," *Trends in Food Science and Technology*, vol. 110, pp. 729–742, 2021.

[23] A. Y. Aydar, *Plant-Based Foods: Ingredients, Technology and Health Aspects*, Springer Nature, New York, NY, USA, 2023.

[24] P. Shanthakumar, J. Klepacka, A. Bains, P. Chawla, S. B. Dhull, and A. Najda, "The current situation of pea protein and its application in the food industry," *Molecules*, vol. 27, no. 16, p. 5354, 2022.

[25] T. Delompré, E. Guichard, L. Briand, and C. Salles, "Taste perception of nutrients found in nutritional supplements: a review," *Nutrients*, vol. 11, no. 9, p. 2050, 2019.

[26] N. D. Patil, A. Bains, K. Sridhar et al., "Enhancing zinc uptake through dual-modification of cicer arietinum protein," *Journal of Food Biochemistry*, vol. 2023, pp. 1–26, 2023.

[27] O. Santosh, H. Kaur Bajwa, M. Singh Bisht, and C. Nirmala, "Functional biscuits from bamboo shoots: enrichment of nutrients, bioactive compounds and minerals in bamboo shoot paste fortified biscuits," *International Journal of Food Science and Nutrition*, vol. 4, pp. 89–94, 2019.

[28] O. H. Lowry, N. J. Rosebrough, A. L. Farr, and R. J. Randall, "Protein measurement with the Folin phenol reagent," *Journal of Biological Chemistry*, vol. 193, no. 1, pp. 265–275, 1951.

[29] T. N. Abduljabbar, B. L. Sharp, H. J. Reid, N. Barzegar-Befroeid, T. Peto, and I. Lengyel, "Determination of Zn, Cu and Fe in human patients' serum using microsampling ICP-MS and sample dilution," *Talanta*, vol. 204, pp. 663–669, 2019.

[30] B. G. Shilpashree, S. Arora, S. Kapila, and V. Sharma, "Physicochemical characterization of mineral (iron/zinc) bound caseinate and their mineral uptake in Caco-2 cells," *Food Chemistry*, vol. 257, pp. 101–111, 2018.

[31] Y. Li, Y. Cheng, Z. Zhang et al., "Modification of rapeseed protein by ultrasound-assisted pH shift treatment: ultrasonic mode and frequency screening, changes in protein solubility and structural characteristics," *Ultrasonics Sonochemistry*, vol. 69, Article ID 105240, 2020.

[32] X. Li, C. Yuan, L. Lu, M. Zhu, S. Xing, and X. Fu, "Exploration of zinc (II) complexes as potent inhibitors against protein

tyrosine phosphatase 1B," *Chemical Research in Chinese Universities*, vol. 35, no. 2, pp. 186–192, 2019.

[33] M. Relucenti, G. Familiari, O. Donfrancesco et al., "Microscopy methods for biofilm imaging: focus on SEM and VP-SEM pros and cons," *Biology*, vol. 10, no. 1, p. 51, 2021.

[34] N. Saadatkhah, A. Carillo Garcia, S. Ackermann et al., "Experimental methods in chemical engineering: thermogravimetric analysis—TGA," *Canadian Journal of Chemical Engineering*, vol. 98, no. 1, pp. 34–43, 2020.

[35] H. Tiernan, B. Byrne, and S. G. Kazarian, "ATR-FTIR spectroscopy and spectroscopic imaging for the analysis of biopharmaceuticals," *Spectrochimica Acta Part A: Molecular and Biomolecular Spectroscopy*, vol. 241, Article ID 118636, 2020.

[36] D. Li, Y. Zhao, X. Wang et al., "Effects of (+)-catechin on a rice bran protein oil-in-water emulsion: droplet size, zeta-potential, emulsifying properties, and rheological behavior," *Food Hydrocolloids*, vol. 98, Article ID 105306, 2020.

[37] X. He, C. Sun, H. Khalesi et al., "Comparison of cellulose derivatives for Ca2+ and Zn2+ adsorption: binding behavior and in vivo bioavailability," *Carbohydrate Polymers*, vol. 294, Article ID 119837, 2022.

[38] M. Jiang, T. Yang, Y. Chu et al., "Design of a novel Pt (ii) complex to reverse cisplatin-induced resistance in lung cancer via a multi-mechanism," *Dalton Transactions*, vol. 51, no. 13, pp. 5257–5270, 2022.

[39] P. Pokharel, Z. Ma, and S. X. Chang, "Biochar increases soil microbial biomass with changes in extra-and intracellular enzyme activities: a global meta-analysis," *Biochar*, vol. 2, no. 1, pp. 65–79, 2020.

[40] M. Cvek, U. C. Paul, J. Zia, G. Mancini, V. Sedlarik, and A. Athanassiou, "Biodegradable films of PLA/PPC and curcumin as packaging materials and smart indicators of food spoilage," *ACS Applied Materials and Interfaces*, vol. 14, no. 12, pp. 14654–14667, 2022.

[41] X. Chen, W. Zhang, S. Y. Quek, and L. Zhao, "Flavor-food ingredient interactions in fortified or reformulated novel food: binding behaviors, manipulation strategies, sensory impacts, and future trends in delicious and healthy food design," *Comprehensive Reviews in Food Science and Food Safety*, vol. 22, no. 5, pp. 4004–4029, 2023.

[42] D. Panáček, L. Zdražil, M. Langer et al., "Graphene nanobeacons with high-affinity pockets for combined, selective, and effective decontamination and reagentless detection of heavy metals (small 33/2022)," *Small*, vol. 18, no. 33, Article ID 2270179, 2022.

[43] L. Wang, Y. Liu, X. Shu, S. Lu, X. Xie, and Q. Shi, "Complexation and conformation of lead ion with poly-γ-glutamic acid in soluble state," *PLoS One*, vol. 14, no. 9, Article ID e0218742, 2019.

[44] B. G. Shilpashree, S. Arora, P. Chawla, and V. Sharma, "A comparison of zinc interactions with succinylated milk protein concentrate and sodium caseinate," *Lebensmittel-Wissenschaft and Technologie*, vol. 157, 2022.

[45] P. Y. Shih, Y. L. Fang, S.-P. Shankar et al., "Phase separation and zinc-induced transition modulate synaptic distribution and association of autism-linked CTTNBP2 and SHANK3," *Nature Communications*, vol. 13, no. 1, Article ID 2664, 2022.

[46] M. Roy, A. K. Nath, I. Pal, and S. G. Dey, "Second sphere interactions in amyloidogenic diseases," *Chemistry Review*, vol. 122, no. 14, pp. 12132–12206, 2022.

[47] X. Qin, J. Zhang, B. Wang et al., "Ferritinophagy is involved in the zinc oxide nanoparticles-induced ferroptosis of vascular endothelial cells," *Autophagy*, vol. 17, no. 12, pp. 4266–4285, 2021.

[48] P. M. Gopinath, V. Saranya, S. Vijayakumar et al., "Assessment on interactive prospectives of nanoplastics with plasma proteins and the toxicological impacts of virgin, coronated and environmentally released-nanoplastics," *Scientific Reports*, vol. 9, no. 1, p. 8860, 2019.

[49] A. Rahman, M. H. Harunsani, A. L. Tan, N. Ahmad, B.-K. Min, and M. M. Khan, "Influence of Mg and Cu dual-doping on phytogenic synthesized ZnO for light induced antibacterial and radical scavenging activities," *Materials Science in Semiconductor Processing*, vol. 128, Article ID 105761, 2021.

[50] J. Zhang, Y. Tang, S. Zhou et al., "Novel strategy to improve the bioactivity and anti-hydrolysis ability of oat peptides via zinc ion-induced assembling," *Food Chemistry*, vol. 416, Article ID 135468, 2023.

[51] V. A. Lushpa, M. V. Goncharuk, C. Lin et al., "Modulation of Toll-like receptor 1 intracellular domain structure and activity by Zn2+ ions," *Communications Biology*, vol. 4, p. 1003, 2021.

[52] B. Zhao, Y. Zhang, B. Sun et al., "Insights into the trace Sr2+ impact on the gel properties and spatial structure of mutton myofibrillar proteins," *Food Research International*, vol. 164, Article ID 112298, 2023.

[53] K. Planeta Kepp, "Bioinorganic chemistry of zinc in relation to the immune system," *ChemBioChem*, vol. 23, no. 9, p. e202100554, 2022.

[54] R. Eivazzadeh-Keihan, H. Bahreinizad, Z. Amiri et al., "Functionalized magnetic nanoparticles for the separation and purification of proteins and peptides," *TrAC, Trends in Analytical Chemistry*, vol. 141, Article ID 116291, 2021.

[55] R. Kornet, J. Yang, P. Venema, E. van der Linden, and L. M. C. Sagis, "Optimizing pea protein fractionation to yield protein fractions with a high foaming and emulsifying capacity," *Food Hydrocolloids*, vol. 126, Article ID 107456, 2022.

[56] E. Lizundia, M. H. Sipponen, L. G. Greca et al., "Multifunctional lignin-based nanocomposites and nanohybrids," *Green Chemistry*, vol. 23, no. 18, pp. 6698–6760, 2021.

[57] M. Duan, T. Li, B. Liu et al., "Zinc nutrition and dietary zinc supplements," *Critical Reviews in Food Science and Nutrition*, vol. 63, no. 9, pp. 1277–1292, 2023.

[58] K. Grüngreiff, T. Gottstein, and D. Reinhold, "Zinc deficiency-an independent risk factor in the pathogenesis of haemorrhagic stroke?" *Nutrients*, vol. 12, no. 11, p. 3548, 2020.

[59] E. Luchinat, M. Cremonini, and L. Banci, "Radio signals from live cells: the coming of age of in-cell solution NMR," *Chemistry Review*, vol. 122, no. 10, pp. 9267–9306, 2022.

[60] F. Nadeem and M. Farooq, "Application of micronutrients in rice-wheat cropping system of south Asia," *Rice Science*, vol. 26, no. 6, pp. 356–371, 2019.

[61] E. Feizollahi, R. S. Mirmahdi, A. Zoghi, R. T. Zijlstra, M. S. Roopesh, and T. Vasanthan, "Review of the beneficial and anti-nutritional qualities of phytic acid, and procedures for removing it from food products," *Food Research International*, vol. 143, Article ID 110284, 2021.

[62] C. Silva, C. Sousa, A. Moutinho, and C. Ferreira Da Vinha, "Trace minerals in human health: iron, zinc, copper, manganese and fluorine," *International Journal of Social Research Methodology*, vol. 13, pp. 57–80, 2019.

[63] M. Saad, L. M. El-Samad, R. A. Gomaa, M. A. Augustyniak, and M. A. Hassan, "A comprehensive review of recent advances in silk sericin: extraction approaches, structure, biochemical characterization, and biomedical applications,"

International Journal of Biological Macromolecules, vol. 250, Article ID 126067, 2023.

[64] A. Mirbolook, M. Rasouli-Sadaghiani, E. Sepehr, A. Lakzian, and M. Hakimi, "Synthesized Zn (II)-amino acid and-chitosan chelates to increase Zn uptake by bean (Phaseolus vulgaris) plants," *Journal of Plant Growth Regulation*, vol. 40, no. 2, pp. 831–847, 2021.

[65] M. Maares and H. Haase, "A guide to human zinc absorption: general overview and recent advances of in vitro intestinal models," *Nutrients*, vol. 12, no. 3, p. 762, 2020.

[66] M. Yadav, N. George, and V. Dwibedi, "Emergence of toxic trace elements in plant environment: insights into potential of silica nanoparticles for mitigation of metal toxicity in plants," *Environmental Pollution*, vol. 333, Article ID 122112, 2023.

[67] K. A. Rahate, M. Madhumita, and P. K. Prabhakar, "Nutritional composition, anti-nutritional factors, pretreatments-cum-processing impact and food formulation potential of faba bean (Vicia faba L.): a comprehensive review," *The Tech*, vol. 138, Article ID 110796, 2021.

[68] L. Passos, P. R. C. Reis, L. C. R. d. S. Lima, F. d. Souza Sobrinho, and J. C. J. d. Silva, "Comparative effects of ammonium and nitrate ions on growth and uptake of multiple elements of ruzigrass," *Journal of Plant Nutrition*, vol. 46, no. 14, pp. 3370–3384, 2023.